



CrossMark
click for updates

Cite this: *RSC Adv.*, 2015, 5, 9574

Concurrence of de-alloying and re-alloying in a ternary Al₆₇Cu₁₈Sn₁₅ alloy and the fabrication of 3D nanoporous Cu–Sn composite structures

T. Song,^a M. Yan,^a Y. Gao,^b A. Atrens^c and M. Qian^{*a}

We report the concurrence of de-alloying and re-alloying in a ternary Al₆₇Cu₁₈Sn₁₅ alloy (at.%) de-alloyed in a 5 wt% hydrochloric acid (HCl) solution at 70 ± 2 °C, and the fabrication of three-dimensional (3D) nanoporous Cu₃Sn–Cu–Cu₆Sn₅ composites in the form of self-supporting foils. Re-alloying occurred in Al₆₇Cu₁₈Sn₁₅ compared to de-alloying alone in binary Al–Cu alloys. Both Cu₃Sn and Cu₆Sn₅ phases formed through an accompanied re-alloying process. This finding further proves the temperature sensitivity of phase formation in the Cu–Sn system established from Cu–Sn diffusion couple studies, and demonstrates the capability of designing and creating nanoporous composite materials *via* de-alloying a multicomponent alloy.

Received 2nd December 2014
Accepted 5th January 2015

DOI: 10.1039/c4ra15622f

www.rsc.org/advances

1. Introduction

De-alloying is the selective dissolution of one or more components from an alloy, leaving behind a material enriched in the nobler or less active alloy component. This approach was used as early as during the Incan civilization to dissolve the more active element Cu from dilute AuCu alloys to create the illusion of a pure gold artefact.¹ The last decade has seen a renewed interest in this approach due to its capability of producing nanoporous structures, which holds promise for applications as sensors^{2,3} and catalysts based on their high specific surface areas.⁴

There are two prerequisites for an alloy to undergo de-alloying:^{5–7} (i) the constituting elements in the alloy should have different electrochemical activities (*e.g.* A is less noble whilst B is nobler in a binary AB alloy);⁵ and (ii) the concentration of the nobler element B is below a critical composition, referred to as parting limit, beyond which de-alloying does not take place due to surface passivation by the nobler element B.^{6,7} Many binary alloys meet these two requirements, including single solid-solution alloys of Au–Ag,⁸ Pt–Co,^{9,10} and Au–Cu,¹¹ and two-phase alloys of Al–Cu,^{12,13} Al–Ag,¹⁴ Zn–Cu¹⁵ and Mg–Cu.^{12,16} They have been de-alloyed to produce nanoporous pure metals, and the mechanisms that control the nanoporosity and pattern formation have been investigated.^{6,7,9,10,12–19} De-alloying of a

binary AB alloy involves the dissolution of A, and the diffusion of B.¹⁷ Both the rate of dissolution of A, and the surface diffusivity of B, have a significant influence on the formation of the nanoporous structure, including the size of the ligaments/channels in the nanoporous B.²⁰

Research on de-alloying over the last decade has been largely focused on de-alloying of binary alloys (AB) with a view to producing nanoporous structures of essentially pure metal B, and understanding the de-alloying process. Only a few studies have dealt with de-alloying of alloys containing a third element such as Mg_{90–x}Cu_xY₁₀,²¹ Mg₇₇Ag_{18.4}Pd_{4.6},²² Ag₆₄Au₃₀Pt₆,²³ Al₇₅Pt₁₅Au₁₀²⁴ and Al₆₆Au_{27.2}X_{6.8} (X = Pt, Pd, PtPd, Ni, Co and NiCo) (in at.%).^{25,26} However, it should be pointed out that in these ternary ABC alloys, the third element C introduced was similar to the nobler element B, a slow diffuser. The purpose was to slow down the surface diffusivity of B, in order to decrease the ligament/channel size of the resulting nanoporous B.^{21–23,26} The small amount of this third element C substituted for the noble element B in the lattice of the precursor alloys.^{21–23,26} Accordingly, de-alloying of these deceptively ternary alloys was no different from the de-alloying of binary alloys.

For de-alloying of ternary alloys (ABC), which consist of three distinctly different elements, the only research reported to date appears to be that by Feng *et al.*²⁷ As with de-alloying of binary AB alloys, which produces nanoporous structures of essentially pure metal B, de-alloying of ternary ABC alloys has the potential to produce nanoporous composite structures with constituting elements B and C and with characteristics different from those de-alloyed from binary alloys for various applications. In addition, de-alloying of ternary alloys is expected to show different dissolution and diffusion behaviors due to the involvement of the third distinctly element. Understanding their de-alloying characteristics is necessary for the fabrication of more

^aRMIT University, School of Aerospace, Mechanical and Manufacturing Engineering, Centre for Additive Manufacturing, Melbourne, VIC 3001, Australia. E-mail: ma.qian@rmit.edu.au

^bShanghai Key Laboratory of Modern Metallurgy and Materials Processing, Shanghai University, 200072 Shanghai, P.R. China

^cThe University of Queensland, Division of Materials, School of Mechanical and Mining Engineering, Brisbane, QLD 4072, Australia

complex nanoporous metal structures aside from enhancing the knowledge base of de-alloying.

This paper studied the de-alloying of a ternary $\text{Al}_{67}\text{Cu}_{18}\text{Sn}_{15}$ alloy at 70 ± 2 °C in a selected acid solution. The rationale for the selection of an AlCuSn ternary alloy is given as follows. First, dense nanostructured intermetallic Cu_6Sn_5 anodes outperform pure Sn anodes in lithium ion batteries, where the inactive Cu matrix can act as a stress buffer to accommodate the large volume change caused by lithiation/delithiation during battery operation.^{28–30} The use of a nanoporous structure has proved to be effective to absorb the volume change of the anode material in lithium ion batteries, such as nanoporous SnO_2 anodes³¹ and nanoporous Ge–C anodes.³² Nanoporous Cu–Sn based composites, if they can be created by de-alloying of a ternary AlCuSn alloy, may have the potential to show desired strain-accommodation capabilities due to their nanoporous structure. In addition, they may offer some good composite strain buffer ability too, like the Sn–Cu composites.^{28–30} Second, Al is electrochemically more active than both Cu and Sn.⁵ This allows the creation of various Cu–Sn based nanostructures *via* the de-alloying of AlCuSn alloys. Third, both Cu and Sn have fast self-diffusion rates,³³ which are in favour of complete de-alloying of the entire sample. Additionally, Cu atoms can diffuse interstitially into Sn even at room temperature to enable intermetallic formation.^{34,35} These characteristics imply that AlCuSn alloys are promising candidate ternary precursors for the creation of a Cu–Sn based nanoporous structure *via* de-alloying of the Al. The composition of the ternary $\text{Al}_{67}\text{Cu}_{18}\text{Sn}_{15}$ alloy was determined as follows. The concentration of 67 at.% Al was chosen to be close to the parting limit of Al^{67} whilst the relative concentrations of Cu and Sn were chosen to match the ratio of 1.2 : 1 for Cu to Sn in Cu_6Sn_5 .³⁰ The selection of the de-alloying temperature (70 ± 2 °C) is based on the phase formation sequence in the Cu–Sn system established from Cu–Sn diffusion couple studies,³⁵ which identified that below 60 °C only Cu_6Sn_5 forms while at or above 60 °C both Cu_6Sn_5 and Cu_3Sn can develop.³⁵ Feng *et al.*²⁷ have recently reported the formation of Cu_6Sn_5 by de-alloying of an $\text{Al}_{10}\text{Cu}_3\text{Sn}$ alloy at 60 °C but no formation of Cu_3Sn was observed. The selection of 70 ± 2 °C is expected to lead to the formation of Cu_3Sn and this will allow us to compare the phase formation in de-alloying with the observations made from diffusion couple studies.

2. Experimental

The $\text{Al}_{67}\text{Cu}_{18}\text{Sn}_{15}$ alloy was prepared from 99.99% purity Al, 99.99% purity Cu and 99.999% purity Sn using arc melting under argon. The alloy was remelted four times to ensure chemical homogeneity. The molten alloy from the fourth remelting was sucked into a water-cooled copper mould with a cavity of 8 mm in diameter and 30 mm in length, by the pressure differential between the mould and melting chamber. Disc samples were cut from the rod, ground and polished into 0.6 mm thick foils (8 mm in diameter).

De-alloying of the foil samples was carried out at 70 ± 2 °C in 200 ml of 5 wt% HCl aqueous solution. A hot plate and a mercurial thermometer were used to control the temperature. According to the preliminary tests performed on three disc

samples, it was found that complete de-alloying of each sample required about 480 min. On this basis, samples were de-alloyed for various durations from 60 min to 480 min. This permitted a systematic study of the de-alloying process. De-alloyed samples were removed from the acid solution, rinsed in distilled water and dehydrated with alcohol.

The phase constitution and microstructure were characterized using X-ray diffraction (XRD, Bruker D8 instrument, with Cu K α radiation, with a scanning rate of 1° min^{-1}), scanning electron microscopy (SEM) in both the second electron (SE) imaging and backscattered electron (BSE) imaging modes (JEOL 7001, operated at 15 keV equipped with energy dispersive X-ray spectroscopy (EDX) made by INCA). Transmission electron microscopy (TEM) and selected area electron diffraction (SAED) (from JEOL 2100, operated at 200 kV) were also employed to study the microstructure and phase constitution. Samples for TEM analysis were prepared by grinding the as-dealloyed foils into powder, followed by dispersing the powder in ethanol by ultrasonic, and finally releasing just a few drops of the particles-containing ethanol solution on a 3 mm diameter carbon film supported on a copper grid. After drying in air for 20 min, the powder samples were ready for TEM analysis.

3. Results

3.1 Phase constitution of precursor

Fig. 1 presents the XRD patterns and a typical SEM micrograph of the precursor $\text{Al}_{67}\text{Cu}_{18}\text{Sn}_{15}$ alloy, which consisted of three phases: α -Al(Cu, Sn) solid solution, β -Sn(Al, Cu) solid solution, and the Al_2Cu intermetallic. At room temperature, the solubility limits of Cu and Sn in Al are 5.5 wt%³⁶ and 0.12 wt%,³⁷ respectively, whilst β -Sn(Al, Cu) contains only up to 0.06 wt% Al and 0.005 wt% Cu.³⁸ Hence, the solid solutions are essentially α -Al(Cu) and metallic β -Sn. Fig. 1 shows the α -Al(Cu) phase (dark contrast), the Al_2Cu phase (grey contrast), and the Sn phase (bright contrast, enveloping the Al_2Cu phase), using the BSE imaging mode. These observations are consistent with the Al–Cu–Sn ternary phase diagram.³⁹

3.2 Phase constitution and morphology evolution during dealloying

The following observations are notable after various durations of de-alloying from 60 to 480 min according to the XRD patterns shown in Fig. 2a and b.

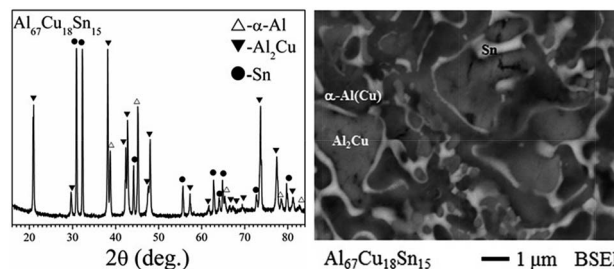


Fig. 1 XRD pattern and SEM BSE microstructure of the $\text{Al}_{67}\text{Cu}_{18}\text{Sn}_{15}$ precursor.

(i) The α -Al(Cu) had disappeared after the first 60 min de-alloying, and there were new phases, identified to be Cu_3Sn , Cu and Cu_6Sn_5 with a preponderance of the Cu_3Sn phase. In addition, there was a noticeable decrease in the intensity of the XRD peaks for both Al_2Cu and Sn. Fig. 3 shows the microstructures after 60 min, 120 min and 180 min de-alloying. The preferential de-alloying of α -Al(Cu) can be seen from Fig. 3a. Fig. 3b shows remnants of Sn and a surface nanoporous structure (with an average ligament width of 40 ± 8 nm) on the Al_2Cu substrate, which is interpreted to be Cu_3Sn and/or Cu according to the XRD results in Fig. 2a and c. With the progress of de-alloying, the nanoporous structure on the Al_2Cu substrate became increasingly coarser (see Fig. 3c and d) while the amount of Cu_3Sn and/or Cu continued to increase (see Fig. 2a).

(ii) No Sn was detected by XRD after 240 min de-alloying, and there was a noticeable decrease in the intensity of the XRD peaks for Al_2Cu . The SEM BSE image in Fig. 4a confirmed the absence of Sn. The surface nanoporous structure after the first 180 min de-alloying (Fig. 3b–d) had further developed after 240 min de-alloying as shown in Fig. 4b. TEM selected area electron diffraction (SAED) identified the presence of both Cu_3Sn and Cu_6Sn_5 (Fig. 4d), consistent with the XRD results.

(iii) The Al_2Cu phase remained after 300 min de-alloying but had disappeared after 480 min de-alloying (Fig. 2b), indicative of complete de-alloying of the Al_2Cu phase. This was confirmed by the microstructures shown in Fig. 5a and b, in which no Al_2Cu was observed. The three strongest XRD lines in the 2θ range of 23 – 47° for each of the Cu_3Sn (JSPDS reference no. 03-065-4653), Cu (00-004-0836) and Cu_6Sn_5 (01-076-2703) phases in the International Centre for Diffraction Data (ICDD) database are shown in Fig. 2c to assist in phase identification.

The microstructure of the final dealloyed product is shown in Fig. 5. A nanoporous microstructure with an average

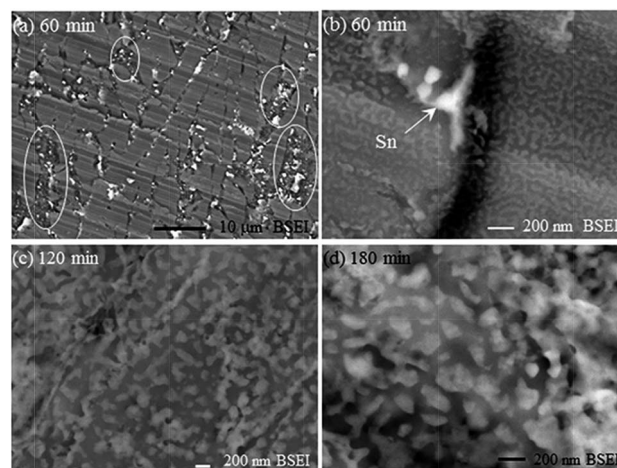


Fig. 3 (a) SEM image showing preferential de-alloying of α -Al(Cu) (circled); (b) remnants of Sn (arrowed) and nanoporous Cu_3Sn and Cu on Al_2Cu substrate; (c) and (d) surface nanoporous structures after 120 min and 180 min de-alloying.

ligament width of 170 ± 50 nm was obtained on the surface (Fig. 5a and b) and throughout the longitudinal section (Fig. 5c and d). The inhomogeneous microstructure observed after 240 min (Fig. 4c) and 300 min de-alloying (Fig. 4e and f) had evolved into a homogenous nanoporous structure (Fig. 5c). TEM examination confirmed the nanoporous nature of the product (Fig. 5e). Also, the existence of Cu_3Sn and Cu_6Sn_5 was identified by SAED and high resolution TEM images (Fig. 5f), consistent

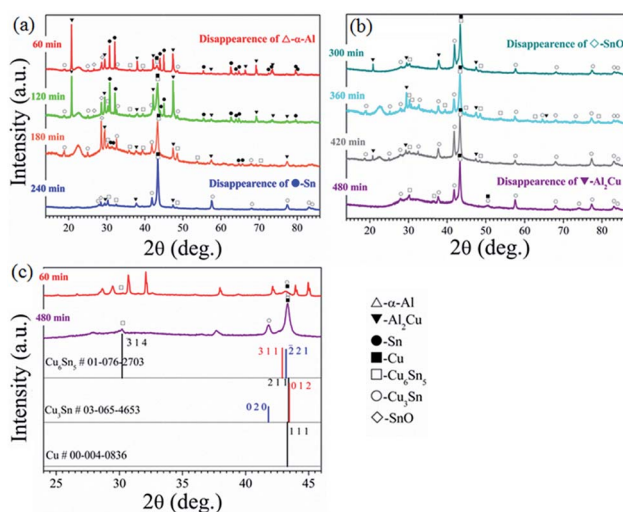


Fig. 2 (a and b) XRD patterns of $\text{Al}_{67}\text{Cu}_{18}\text{Sn}_{15}$ alloy after de-alloying in a 5 wt% HCl solution for up to 480 min; and (c) three strongest diffraction lines (in 2θ range of 23 – 47°) for each of the Cu_3Sn , Cu and Cu_6Sn_5 phases in the ICDD database together with XRD patterns obtained from samples after 60 and 480 min de-alloying.

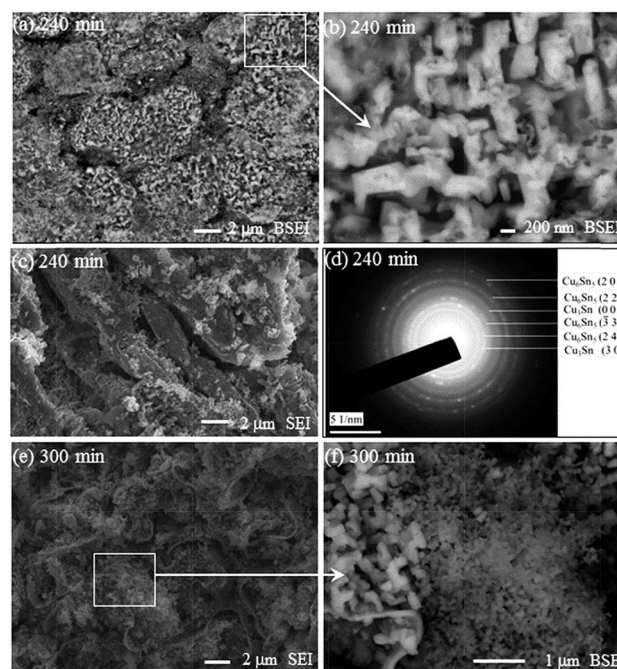


Fig. 4 (a) and (b) surface nanoporous structures of Cu_3Sn – Cu – Cu_6Sn_5 ; (c) inhomogeneous microstructure on cross section; (d) TEM SAED results of Cu_3Sn and Cu_6Sn_5 after 240 min de-alloying; and (e) and (f) inhomogeneous microstructure after 300 min of de-alloying.

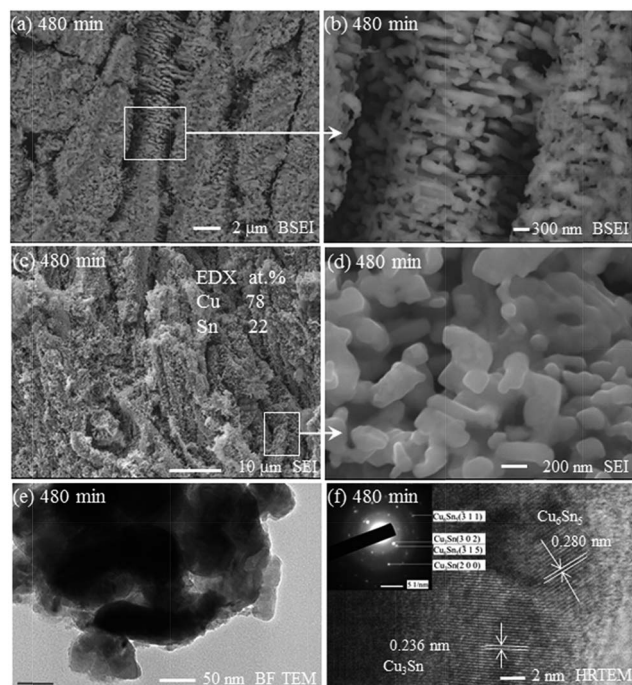


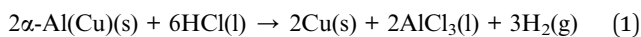
Fig. 5 Nanoporous structures of $\text{Cu}_3\text{Sn}-\text{Cu}-\text{Cu}_6\text{Sn}_5$ produced after 480 min de-alloying: (a) and (b) surface; (c) and (d) cross section; (e) bright field (BF) TEM image confirming the nanoporous structure; and (f) HRTEM image and TEM SAED results of Cu_3Sn and Cu_6Sn_5 phases. The nanoporous $\text{Cu}_3\text{Sn}-\text{Cu}-\text{Cu}_6\text{Sn}_5$ composite is produced in the form of self-supporting foils (0.6 mm thick and 8 mm in diameter).

with the XRD results. EDX analyses detected no Al but did detect Cu and Sn (as presented in the inset in Fig. 5c). In addition, the atomic ratio of Cu : Sn detected by EDX analyses is around 78 : 22, which is clearly greater than the ratio of Cu to Sn in either Cu_3Sn (3 : 1) or Cu_6Sn_5 (1.2 : 1.0). This supports the detection of free Cu in the de-alloyed sample by XRD. The nanoporous $\text{Cu}_3\text{Sn}-\text{Cu}-\text{Cu}_6\text{Sn}_5$ composite is produced in the form of self-supporting foils (0.6 mm thick and 8 mm in diameter).

4. Discussion

4.1 De-alloying of ternary AlCuSn alloys

$\alpha\text{-Al}(\text{Cu})$ has a large volume fraction in the precursor ternary $\text{Al}_{67}\text{Cu}_{18}\text{Sn}_{15}$ alloy (Fig. 1). De-alloying of the $\text{Al}_{67}\text{Cu}_{18}\text{Sn}_{15}$ alloy started with the preferential dissolution of $\alpha\text{-Al}(\text{Cu})$, as evidenced by its quick disappearance after 60 min de-alloying (Fig. 2a). This is similar to the observations made from the de-alloying of other Al-based alloys (binary $\text{Al}_{65}\text{Ag}_{35}$,¹⁴ AlCu ,^{12,13,40,41} or ternary $\text{Al}_{66}\text{Au}_{27.2}\text{X}_{6.8}$ (X = Pt, Pd, PtPd, Ni, Co and NiCo)²⁶). It was noticed that there was release of hydrogen (H_2) as gas bubbles during de-alloying. Hence the de-alloying process of the $\alpha\text{-Al}(\text{Cu})$ phase may be described as follows



where the Cu atoms released from this process are limited to the solubility of Cu in $\alpha\text{-Al}$.

De-alloying of the Al_2Cu phase also occurred in this process, as informed by the notable decrease in the intensity of the Al_2Cu XRD peaks. Considering both the release of H_2 and the presence of free Cu in the final de-alloyed product, the de-alloying process of Al_2Cu may be described by eqn (2) below



As mentioned previously, the only other study of de-alloying of ternary AlCuSn alloys was that by Feng *et al.*²⁷ Table 1 lists the distinct differences between this study and Feng *et al.*'s work.²⁷

(i) **Different precursors.** The precursor used in ref. 27 was based on Cu_3Sn while this study is based on Cu_6Sn_5 (18 : 15 = 6 : 5) aiming to obtain a nanoporous Cu_6Sn_5 , as the Cu_6Sn_5 compound has proved to outperform pure Sn as anode material.^{28,29}

(ii) **Different electrolyte solutions.** Both NaOH and HCl solutions are able to dissolve Al from Al-based alloys for de-alloying.^{12–14,24,40,41} The selection of HCl solutions is complementary to the selection of NaOH solutions for the de-alloying of AlCuSn alloys²⁷ and it can also show the influence of electrolyte on the de-alloying of AlCuSn alloys.

(iii) **Different de-alloying temperatures.** Detailed Cu–Sn diffusion couple studies have indicated that below 60 °C only Cu_6Sn_5 forms while at or above 60 °C both Cu_6Sn_5 and Cu_3Sn can form.³⁵ Indeed, Feng *et al.*²⁷ selected 60 °C and confirmed only the formation of Cu_6Sn_5 although the ratio of Cu : Sn of their precursor was designed to be 3 : 1. In contrast, by selecting 70 ± 2 °C, both Cu_6Sn_5 and Cu_3Sn formed during de-alloying, consistent with Cu–Sn diffusion couple studies.³⁵

As a result of the differences discussed above, Feng *et al.* obtained nanoporous Cu– Cu_6Sn_5 (ref. 27) while this study attained nanoporous $\text{Cu}_3\text{Sn}-\text{Cu}-\text{Cu}_6\text{Sn}_5$. These two different studies are complementary to each other and together they show the significances of precursor composition, electrolyte type, and de-alloying temperature in the de-alloying process of ternary AlCuSn alloys. Also noticed from the XRD results shown in Fig. 2a and b is a small presence of the SnO phase in the samples de-alloyed for 60–300 min. This can be attributed to oxidation in the de-alloying solution. However, no SnO phase was detected after de-alloying for 300 min (Fig. 2b). The consumption of Sn by oxidation could be one of the reasons responsible for the lower Sn content in the final product of $\text{Cu}_3\text{Sn}-\text{Cu}-\text{Cu}_6\text{Sn}_5$ than in the precursor alloy.

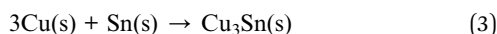
4.2 Re-alloying of Cu and Sn among de-alloying

The XRD results together with the ICDD information (Fig. 2) revealed that, there was formation of both Cu_3Sn and Cu_6Sn_5

Table 1 De-alloying of ternary AlCuSn alloys

De-alloying system	Feng <i>et al.</i> 's paper ²⁷	This study
Precursor composition (at.%)	$\text{Al}_{10}\text{Cu}_3\text{Sn}$	$\text{Al}_{67}\text{Cu}_{18}\text{Sn}_{15}$
Electrolyte solution	20 wt% NaOH	5 wt% HCl
De-alloying temperature (°C)	60	70 ± 2
De-alloyed product	$\text{Cu}-\text{Cu}_6\text{Sn}_5$	$\text{Cu}_3\text{Sn}-\text{Cu}-\text{Cu}_6\text{Sn}_5$

during de-alloying at 70 ± 2 °C from the early stages (60 min) of de-alloying to the end (480 min). This means that there has been re-alloying that occurred between the Cu atoms released from reactions (1) and (2) and the Sn atoms in the precursor. These re-alloying processes may be described by eqn (3) and (4) below.

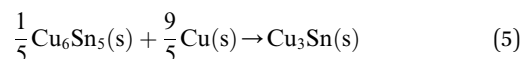


It has long been established that at room temperature, Cu atoms can diffuse fast (interstitially) into the lattice of Sn, particularly along the *c*-axis direction in the lattice of Sn,³⁴ and then react with Sn to form Cu_6Sn_5 .^{35,42,43} This occurs at room temperature and from the formation of many other intermetallic compounds which typically occurs at a much higher temperature. The free Cu atoms released by de-alloying according to eqn (1) and (2) were expected to be chemically reactive, as would also be the newly exposed Sn atoms in the precursor alloy. In addition, the de-alloying or removal of the Al atoms from the ternary precursor alloy $\text{Al}_{67}\text{Cu}_{18}\text{Sn}_{15}$ naturally left Cu and Sn atoms in contact. This enables the formation of Cu_6Sn_5 and Cu_3Sn during de-alloying at 70 ± 2 °C. The formation of Cu_3Sn and Cu_6Sn_5 is based on the interactions between Cu and Sn atoms, similar to the recent study of dealloying of ternary Al–Au–M (M = Ni, Co or NiCo) alloys by Zhang *et al.*,²⁵ who discussed the importance of the interactions between Au and other atoms. Our study supports Tu's observation³⁵ that "the ordered ϵ -phase (Cu_3Sn) was found only in those specimens that had been annealed above 60 °C", although no experimental data were given by Tu. It has been found that there was formation of just Cu_6Sn_5 during de-alloying of a ternary $\text{Al}_{10}\text{Cu}_3\text{Sn}$ alloy in a 20 wt% NaOH solution at 60 °C.²⁷

Table 2 lists the detailed literature data on intermetallic formation in the Cu–Sn system under various conditions

together with the experimental observations of this study. Previous Cu–Sn diffusion couple studies have established that Cu_6Sn_5 can form over a wide range of temperatures^{3,27,35,42–44,46,47} down to -2 °C (Table 2) while Cu_3Sn forms mainly at temperatures above 100 °C.^{35,42–44,46,47} Dreyer *et al.*³ reported that Cu_3Sn nucleated at the temperature of 87 °C in their Cu/ Cu_6Sn_5 thin film diffusion couple study. It is clear from Table 2 that the formation of Cu_3Sn at 70 ± 2 °C observed in this study is the lowest temperature reported to date for the intermetallic formation of Cu_3Sn with solid experimental data. This improves the knowledge base of phase formation in the Cu–Sn system. Experimental studies have further established that once nucleated, the apparent activation energy (E_a) for the growth of Cu_3Sn ($70.28 \text{ kJ mol}^{-1}$), determined over the temperature range of 120–200 °C, is smaller than that for the growth of Cu_6Sn_5 (84.3 kJ mol^{-1} determined over the temperature range of 70–200 °C).⁴⁸ This implies that Cu_3Sn tends to grow easier than Cu_6Sn_5 . The preponderance of Cu_3Sn over Cu_6Sn_5 in the de-alloyed product can be attributed to this reason.

After the disappearance of Sn, de-alloying of Al_2Cu continued to release free Cu atoms by reaction (2). However, because of the absence of Sn, reactions (3) and (4) no longer occurred. The Cu–Sn diffusion couple studies at temperatures above 100 °C have identified another reaction, described by reaction (5) below,^{35,45,49} for the formation and continued growth of Cu_3Sn in Cu–Sn diffusion couples.



It is plausible that the same reaction may have also occurred in the de-alloying process studied contributing to the preponderance of Cu_3Sn over Cu_6Sn_5 in the final de-alloyed nanoporous Cu_3Sn –Cu– Cu_6Sn_5 structures. However, the noticeable presence of both Cu and Cu_6Sn_5 detected by XRD after 480 min

Table 2 Intermetallic formation in the Cu–Sn system

Diffusion couple	Temperature (°C)	Duration	Intermetallic compounds	Ref.
Cu/Sn	-2^a	NA	Cu_6Sn_5	42
Cu/Sn	Room temperature	15 days	Cu_6Sn_5	42
Cu/Sn	Room temperature	One year	Cu_6Sn_5	42 and 43
Cu/Sn	Room temperature	10 days	Cu_6Sn_5	35
Cu/Sn	60^a	NA	Cu_6Sn_5 and Cu_3Sn	42
Cu/Sn (de-alloying of $\text{Al}_{10}\text{Cu}_3\text{Sn}$)	60	8 h	Cu_6Sn_5	27
Cu/Sn (de-alloying of $\text{Al}_{67}\text{Cu}_{18}\text{Sn}_{15}$)	70 ± 2	60 min	Cu_6Sn_5 and Cu_3Sn	This study
Sn–5Bi–3.5Ag solder/Cu	70, 100 and 120	30 days	Cu_6Sn_5	44
Cu/Sn	87	NA	Cu_3Sn nucleation	3
Cu/Sn	100	36 h	Cu_6Sn_5 and Cu_3Sn	42 and 43
Cu/Sn	100	60 h	Cu_6Sn_5 and Cu_3Sn	42
SnPb solder/ Cu_6Sn_5 / Cu_3Sn /Cu	100, 125 and 150	80 days	Cu_6Sn_5 and Cu_3Sn	45
Lead-free solder/Cu	100, 125, 150 and 170	>50 h	Cu_6Sn_5 and Cu_3Sn	46
Cu/ Cu_6Sn_5	115–150	10 min	Cu_6Sn_5 and Cu_3Sn	35
Lead-free solder/Cu	150	NA	Cu_6Sn_5 and Cu_3Sn	47
Sn–5Bi–3.5Ag solder/Cu	150, 170 and 200	30 days	Cu_6Sn_5 and Cu_3Sn	44
Cu/Sn	200	10 min	Cu_3Sn	35 and 43
SnPb solder/Cu	220	3–4 min	Cu_6Sn_5 and Cu_3Sn	45

^a Without experimental data. NA: not available.

de-alloying suggests that reaction (5) may have only occurred to a small extent by the end of the 480 min de-alloying process. The two predominant reasons are: (i) reaction (5) is slow; it has been found that a large amount of residual Cu_6Sn_5 and Cu still remained after even 80 days of annealing at $150\text{ }^\circ\text{C}$,⁴⁵ and (ii) the de-alloying temperature ($70 \pm 2\text{ }^\circ\text{C}$) used is inadequate to completely overcome the large energy barrier (95.5 kJ mol^{-1} , determined over the temperature range of $115\text{--}150\text{ }^\circ\text{C}$)³⁵ required for reaction (5) to occur. In fact, it is ideal to have a noticeable presence of Cu in the as-dealloyed product as Cu offers better thermal and electrical conductivities than both Cu_6Sn_5 and Cu_3Sn ,^{35,42} in addition to the much needed ductility to hold Cu_6Sn_5 and Cu_3Sn together. In this regard, it is desired that reaction (5) is slow.

5. Conclusions

A ternary $\text{Al}_{67}\text{Cu}_{18}\text{Sn}_{15}$ alloy has been designed and de-alloyed in a 5 wt% hydrochloric acid solution at $70\text{ }^\circ\text{C}$. Unlike de-alloying of binary alloys, de-alloying of the ternary $\text{Al}_{67}\text{Cu}_{18}\text{Sn}_{15}$ alloy was accompanied by a re-alloying process. Together they have enabled the fabrication of a nanoporous $\text{Cu}_3\text{Sn}\text{--Cu--Cu}_6\text{Sn}_5$ composite with an average ligament width of $170 \pm 50\text{ nm}$. The formation of Cu_3Sn and Cu_6Sn_5 intermetallics and the reaction between Cu_6Sn_5 and Cu during de-alloying at $70 \pm 2\text{ }^\circ\text{C}$ are discussed in detail in relation to the experimental findings obtained from the Cu–Sn diffusion couple studies. This finding further proves the temperature sensitivity of phase formation in the Cu–Sn system established from Cu–Sn diffusion couple studies. De-alloying of multicomponent alloys offers an effective approach to the fabrication of nanoporous composite materials including the formation of new phases through the accompanied re-alloying process.

Acknowledgements

T. Song is financially supported by a China Scholarship Council (CSC) Scholarship and a RMIT fee waiver scholarship. Y. Gao acknowledges the Program for Professor of Special Appointment (Eastern Scholar) at Shanghai Institutions of Higher Learning (no. TP2014042).

Notes and references

- H. Lechtman, *Sci. Am.*, 1984, **250**, 63156.
- Y. Wang, J. Cao, S. Wang, X. Guo, J. Zhang, H. Xia, S. Zhang and S. Wu, *J. Phys. Chem. C*, 2008, **112**, 17804.
- K. F. Dreyer, W. K. Neils, R. R. Chromik, D. Grosman and E. J. Cotts, *Appl. Phys. Lett.*, 1995, **67**, 2795.
- T. Déronzier, F. Morfin, L. Massin, M. Lomello and J.-L. Rousset, *Chem. Mater.*, 2011, **23**, 5287.
- H. W. Pickering and C. Wagner, *J. Electrochem. Soc.*, 1967, **114**, 698.
- D. Artymowicz, R. Newman and J. Erlebacher, *ECS Trans.*, 2007, **3**, 499.
- D. M. Artymowicz, J. Erlebacher and R. C. Newman, *Philos. Mag.*, 2009, **89**, 1663.
- K. Zhang, X. Tan, J. Zhang, W. Wu and Y. Tang, *RSC Adv.*, 2014, **4**, 7196.
- L. Liu, E. Pippel, R. Scholz and U. Gosele, *Nano Lett.*, 2009, **9**, 4352.
- Z. Yu, J. Zhang, Z. Liu, J. M. Ziegelbauer, H. Xin, I. Dutta, D. A. Muller and F. T. Wagner, *J. Phys. Chem. C*, 2012, **116**, 19877.
- A. Pareek, G. N. Ankah, S. Cherevko, P. Ebbinghaus, K. J. J. Mayrhofer, A. Erbe and F. U. Renner, *RSC Adv.*, 2013, **3**, 6586.
- W. B. Liu, S. C. Zhang, N. Li, J. W. Zheng, S. S. An and Y. L. Xing, *Corros. Sci.*, 2012, **58**, 133.
- W. B. Liu, S. C. Zhang, N. Li, J. W. Zheng and Y. L. Xing, *Corros. Sci.*, 2011, **53**, 809.
- T. T. Song, Y. L. Gao, Z. H. Zhang and Q. J. Zhai, *Corros. Sci.*, 2013, **68**, 256.
- J. F. Li, P. A. Agyakwa and C. M. Johnson, *Acta Mater.*, 2011, **59**, 1198.
- C. Zhao, X. Wang, Z. Qi, H. Ji and Z. Zhang, *Corros. Sci.*, 2010, **52**, 3962.
- J. Erlebacher, M. J. Aziz, A. Karma, N. Dimitrov and K. Sieradzki, *Nature*, 2001, **410**, 450.
- I. C. Oppenheim, D. J. Trevor, C. E. D. Chidsey, P. L. Trevor and K. Sieradzki, *Science*, 1991, **254**, 687.
- F. U. Renner, A. Stierle, H. Dosch, D. M. Kolb, T. L. Lee and J. Zegenhagen, *Nature*, 2006, **439**, 707.
- Z. Zhang, Y. Wang, Y. Wang, X. Wang, Z. Qi, H. Ji and C. Zhao, *Scr. Mater.*, 2010, **62**, 137.
- X. Luo, R. Li, L. Huang and T. Zhang, *Corros. Sci.*, 2013, **67**, 100.
- H. Ji, X. Wang, C. Zhao, C. Zhang, J. Xu and Z. Zhang, *CrystEngComm*, 2011, **13**, 2617.
- J. Snyder, P. Asanithi, A. B. Dalton and J. Erlebacher, *Adv. Mater.*, 2008, **20**, 4883.
- Z. Zhang, Y. Wang and X. Wang, *Nanoscale*, 2011, **3**, 1663.
- Z. Zhang, C. Zhang, Y. Gao, J. Frenzel, J. Sun and G. Eggeler, *CrystEngComm*, 2012, **14**, 8292.
- Y. Wang, J. Xu and B. Wu, *Phys. Chem. Chem. Phys.*, 2013, **15**, 5499.
- Y. Feng, S. Zhang, Y. Xing and W. Liu, *J. Mater. Sci.*, 2012, **47**, 5911.
- H. C. Shin and M. Liu, *Adv. Funct. Mater.*, 2005, **15**, 582.
- D. Reyter, S. Rousselot, D. Mazouzi, M. Gauthier, P. Moreau, B. Lestriez, D. Guyomard and L. Roué, *J. Power Sources*, 2013, **239**, 308.
- S. Wang, W. Zhao, X. Liu and L. Li, *RSC Adv.*, 2013, **3**, 18339.
- Z. P. Guo, G. D. Du, Y. Nuli, M. F. Hassan and H. K. Liu, *J. Mater. Chem.*, 2009, **19**, 3253.
- J. Cheng, J. Wang, W. Li, X. Liu and Y. Yu, *RSC Adv.*, 2014, **4**, 37746.
- E. G. Seebauer and C. E. Allen, *Prog. Surf. Sci.*, 1995, **49**, 265.
- B. F. Dyson, T. R. Anthony and D. Turnbull, *J. Appl. Phys.*, 1967, **38**, 3408.
- K. N. Tu and R. D. Thompson, *Acta Metall.*, 1982, **30**, 947.
- Y. Kim and R. Buchheit, *Corrosion and Protection of Light Metal Alloys: Proceedings of the International Symposium*, 2004, vol. 23, p. 19.

- 37 A. J. McAlister and D. J. Kahan, *Bull. Alloy Phase Diagrams*, 1983, **4**, 410.
- 38 I. Isaichev, *Zh. Tekh. Fiz.*, 1939, **9**, 1867–1872.
- 39 J. Andrew and C. Edwards, *J. Inst. Met.*, 1909, **11**, 29.
- 40 W. B. Liu, S. C. Zhang, N. Li, J. W. Zheng and Y. L. Xing, *Microporous Mesoporous Mater.*, 2011, **138**, 1.
- 41 W. Liu, S. Zhang, N. Li, J. Zheng and Y. Xing, *J. Electrochem. Soc.*, 2010, **157**, D666.
- 42 K. N. Tu, *Acta Metall.*, 1973, **21**, 347.
- 43 K. N. Tu, *Mater. Chem. Phys.*, 1996, **46**, 217.
- 44 J. W. Yoon, C. B. Lee and S. B. Jung, *Mater. Sci. Technol.*, 2003, **19**, 1101.
- 45 K. Zeng, R. Stierman, T.-C. Chiu, D. Edwards, K. Ano and K. N. Tu, *J. Appl. Phys.*, 2005, **97**, 0245081.
- 46 Y. G. Lee and J. G. Duh, *J. Mater. Sci.: Mater. Electron.*, 1999, **10**, 33.
- 47 Y. G. Lee and J. G. Duh, *J. Mater. Sci.*, 1998, **33**, 5569.
- 48 J.-W. Yoon, C.-B. Lee and S.-B. Jung, *Mater. Sci. Technol.*, 2003, **19**, 1101.
- 49 C. N. Liao and C. T. Wei, *J. Electron. Mater.*, 2004, **33**, 1137.